Journal Name

ARTICLE

4MBA-labeled Ag-nanorod aggregates by coated with SiO₂: synthesis, SERS activity, and biosensing application

Wei Lai,[a] Jun Zhou,[* a] Yanting Liu,[a] Zhenhong Jia,[b] Shusen Xie,[c] Lucia Petti[d] and Pasquale Mormile[d]

A new nanostructure, silica-coated Ag nanorods (NRs) aggregates with 4-mercaptobenzoic acid molecules (4MBA-Ag NRs@SiO₂), was prepared by the seed-mediated growth method and the modified Stöber method. In the synthetic process, the optimal 4MBA-Ag NRs@SiO₂ was obtained by using the different conditions such as surfactant concentration and centrifugation cycles. The morphologies and the optical properties of the 4MBA-Ag NRs@SiO₂ were investigated in detail by the transmission electron microscope, UV-Vis spectrometer and Raman spectrometer. The experimental results show that the 4MBA-Ag NRs@SiO₂ prepared at 0.05 M CTAB has the aggregate morphology of single-crystalline Ag NRs, typical localized surface plasmon resonance (LSPR) characteristic and high enhancement factor of surface-enhanced Raman scattering (SERS). Based on the SERS activity of 4MBA-Ag NRs@SiO₂ and Ag NRs, the immune probe and the immune substrate immobilized with anti-prostate specific antigen (anti-PSA) antibody have been fabricated and used to construct the sandwich structure for the immunoassay of PSA, and the detection limit of PSA had reached to 0.3 fg·ml⁻¹. It is demonstrated the as-prepared 4MBA-Ag NRs@SiO₂ has great potential in the biosensing applications.

Introduction

Since the Bence-Jones protein[1] was found as a tumour marker of multiple myeloma in 1845, a wide variety of hormonic and proteinic type of tumour markers have been subsequently found, such as adrenocorticotropic hormone,[2] carbohydrate antigen 19-9 (CA19-9),[3] and carcinoembryonic antigen (CEA).[4] Especially, α-fetoprotein[5] and prostate-specific antigen[6] as tumour markers have played an important role for early diagnosis, therapy and trace of liver cancer and prostate cancer, respectively. Based on the above facts, it is desirable to develop a highly-sensitive method to precisely detect the tumour markers. The immunoassay is expected to be one of the most useful methods,[7] for example, chemiluminescent immunoassay,[8] paramagnetic particles immunoassay,[9] enzyme linked immunosorbent assay (ELISA),[10] amperometric immunoassay (AI),[11] and fibre-optic localized surface plasmon resonance (LSPR) label-free immunoassay.[12] Though these conventional methods have been widely applied in clinical tests, they are involved the excess consumption of time and money which restrict their application for general survey of cancer.

Recently, the immunoassay based on surface-enhanced Raman scattering (SERS) has been favoured by major researchers due to its high sensitivity, unique spectroscopic fingerprint, and nondestructive data acquisition.[13] Similar to the case of ELISA,[10] a typical strategy of SERS-based immunoassay was used to detect the concentration of apolipoprotein B[14] and IgGs[15] by using the sandwich structure consisted of the nano-Au immune probes with Raman reporter molecules, target antigen and the nano-Ag immune substrate. And a range of the SERS-based nanostructures have been provided and exhibited sufficiently low limit of detection for tumour markers, for example, thiol modified Fe₃O₄@Ag SERS probe,[16] cysteine modified gold nanoparticles,[17] and Silver nanocubes.[18] As we know, the well-shaped Ag nanoparticles (NPs) (Sun et al. 2003) exhibit better SERS performance comparing to their solid block counterparts. However, the poor biocompatibility and instability of Ag NPs have greatly prevented their further applications in biomedical field.[19, 20] Naturally, it is meaningful to use silica as a capping agent of Ag NPs for obtaining a new kind of immune probe with high-sensitivity and excellent biocompatibility.

In this paper, a silica-coated Ag NRs aggregate with 4MBA (4MBA-Ag NRs@SiO₂) was fabricated via the seed-mediated growth method and the modified Stöber method,[21-23] and the as-prepared 4MBA-Ag NRs@SiO₂ exhibits an excellent SERS performance. Furthermore, the immune probe and the immune substrate were fabricated by immobilizing the anti-PSA antibody on the 4MBA-Ag NRs@SiO₂ and the quartz slide with Ag NRs, respectively. A sandwich immunoassay structure consisted of the immune probes/target protein/immune-substrate is used for the specific immunoassay of the prostate-specific antigen (PSA). Our

a. *Institute of Photonics, Faculty of Science, Ningbo University, Ningbo 315211, China. Tel: +86-574-87600794; Fax: +86-574-87600744; *corresponding author E-mail: zhoujun@nbu.edu.cn*
b. *School of Information Science and Engineering, Xinjiang University, Urumqi 830046, China.*
c. *Key Laboratory of Optoelectronic Science & Technology for Medicine of Ministry of Education, Fujian Normal University, Fuzhou 350007, Fujian, China*
d. *Institute of Cybernetics "E. Caianiello" of CNR, Via Campi Flegrei 34, 80072 Pozzuoli, Ital.*

† Electronic Supplementary Information (ESI) available: The immunoassay protocol, High sensitive immunoassay, and SERS active of the sample.

experimental results show that the proposed immunoassay strategy has high sensitivity for detection of PSA.

Experimental

Chemicals

Silver nitrate ($AgNO_3$), 1-(3-Dimethylaminopropyl)-3-ethylcarbodiimide hydrochloride (EDC), Hexadecyl trimethyl ammonium Bromide (CTAB), N-Hydroxysuccinimide (NHS), and 4-mercaptobenzoic acid (4MBA) were purchased from Sigma Aldrich. Sodium borohydride ($NaBH_4$) and ammonia solution ($NH_3·H_2O$) were purchased from Sinopharm Chemical Reagent Co. (Shanghai, China). Trisodium citrate and ascorbic acid (AA) were purchased from Tianjin Bodi Chemical Co. (Tianjin, China). Sodium hydroxide (NaOH) was purchased from Zhejiang Zhongxing Chemical Reagent Co. (Zhejiang, China). Tetraethoxysilane (TEOS) was purchased from J&K Chemical. Ethanol (C_2H_6O) was purchased from Anhui Ante biochemistry Co. (Anhui, China). Prostate-specific antigen (PSA), anti-PSA antibody, apolipoprotein B and Bovine Serum Albumin (BSA) were purchased from Sigma Aldrich. Phosphate buffered solution (PBS, pH 7.0), Tris-buffer solution (TBS, pH 7.6) and TBS/0.05% Tween20 buffer solution (0.05 M Tris, 0.138 M NaCl, 0.0027 M KCl, 0.05% Tween®20, pH 8.0) were also purchased from Sigma Aldrich. Deionized water (Millipore Milli-Q grade) with resistivity of 18.2 MΩ·ml⁻¹ was used to prepare all solutions. All chemicals were the analytical grade and used as received.

Preparation of Ag NRs

Ag NRs were synthesized by the seed-mediated growth method.[21, 22] Briefly, the seed solution was prepared by adding 0.6 ml freshly prepared ice-cold 0.01M $NaBH_4$ solution (reducing agent) into 20 ml mixture solution containing 0.25 mM $AgNO_3$ and 0.25 mM trisodium citrate, under stirring vigorously for 30 s. And the colour of Ag seed solution appeared pale yellow immediately. After left undistructed for 2 h, the as-prepared seed solution should be used within 24 h. Subsequently, the growth solution was prepared by mixing 10.00 ml different concentrations of CTAB (0.02, 0.05 and 0.08 M), 0.4 ml of 0.01 M $AgNO_3$, 0.75 ml of 0.01 M AA and 0.30 ml of 1 M NaOH. Then, three same amount of seed solutions (0.4 ml) were respectively added into the above three growth solutions and gently agitated for 2 min. Finally, the colour of the reaction solutions changed to green, which indicated that Ag NRs were prepared successfully. To remove the excess CTAB in the aqueous solutions, the three Ag NRs solutions were centrifuged consecutively two times at 8,000 rpm for 30 min and dispersed in 12 ml of deionized water, respectively.

Preparation of 4MBA-Ag NRs@SiO₂

The 4MBA-Ag NRs@SiO₂ was prepared as following processes. Firstly, the 4MBA-tagged Ag NRs solution was synthesized by added 10 μl of 1.0 mM 4MBA ethanol solution into the aliquot of the purified Ag NRs solution obtain at different conditions (0.02, 0.05 and 0.08 M CTAB) under stirring and left undisturbed for 12 h.

Then, the unbound 4MBA molecules were removed by centrifuging at 8,000 rpm for 30 min, and the 4MBA-tagged Ag NRs settled to the bottom were dispersed in 2 ml deionized water. Secondly, by using the modified Stöber method,[22] 2 ml absolute ethanol and 20 μl of 27-30% $NH_3·H_2O$ were added into 2 ml the 4MBA-tagged Ag NRs solution under stirring and agitated for 2 min. Then, the same amounts of TEOS (20 μl) were added to the above mixture solutions under stirring for 3 h to form the 4MBA-Ag NRs@SiO₂ solutions. Next, the 4MBA-Ag NRs@SiO₂ solutions were purified by centrifugation at 6000 rpm for 30 min, and the centrifuged precipitates was dispersed into the absolute ethanol. After going through two washing steps, the resultant sediments 4MBA-Ag NRs@SiO₂ were dispersed in 2 ml of PBS solution (pH=7.0) as samples 1, 2, and 3 which corresponding to the above synthesized condition of 0.02, 0.05 and 0.08 M CTAB, respectively.

Preparation of the immune probe

The 4MBA-Ag NRs@SiO₂ immune probes were prepared by a typical modified process. Firstly, the anti-PSA antibody (50 μl, 0.3 ug·ml⁻¹) was added into 0.24 ml PBS solution containing 0.4 mg EDC and 0.2 mg NHS under stirring for 15 min. Secondly, the above mixture solution was added to 1 ml as-prepared 4MBA-Ag NRs@SiO₂ solution under agitating for 2 min. Thirdly, after incubated at 4 °C for 3 h, the resultant solution was centrifuged at 10000 rpm for 20 min to remove the unbound anti-PSA antibody. Lastly, the sediment was dispersed in the 2 ml PBS solution as the 4MBA-Ag NRs@SiO₂ immune probes.

Preparation of the immune substrate

The following three steps were designed to fabricate immune substrate. Firstly, a quartz slide was ultrasonically cleaned with acetone and deionized water for 15 min, respectively, and then dried in air; next, the cleaned quartz slide was immersed in the PDDA solution for 10 min to obtain the positively charged slide, then, the quartz slide was taken out and washed thrice with deionized water; subsequently, the purified Ag NRs solution was dripped to the positively charged slide to form the SERS substrate. Secondly, a certain amount of the anti-PSA antibody (0.3 μg·ml⁻¹) was pipetted onto the SERS substrate and incubated 4 °C for 3 h in an environment with a relative humidity of 60%; next, the as-prepared substrate was washed by PBS solution to remove the excess protein and dried in argon gas so that a monolayer of anti-PSA antibody was immobilized onto the SERS substrate as an immune substrate. Thirdly, the naked Ag NRs on the surface of immune substrate were blocked by the PBS solution with 3% BSA for 3 h at room temperature; next, the immune substrate was continuously washed with TBS/0.05% Tween®20 buffer solution, TBS and deionized water to remove the residual BSA and dried in argon gas atmosphere. Finally, the as-prepared immune substrate was stored at 4 °C for further use.

Immunoassay protocol

The immunoassay of PSA was performed by a sandwich structure consisted of the immune probes/ PSA protein/ the immune substrate, as illustrated in Fig. S1. Firstly, the different amounts of target

antigen (PSA, 0.3 fg ~ 3 μg·ml⁻¹) were dripped onto the as-prepared immune substrates and incubated at room temperature for 3 h. After completing immunoreaction between anti-PSA antibody and PSA, the substrates were continuously rinsed with TBS/0.05% Tween 20 buffer solution, TBS and deionized water to remove any residual PSA that was not captured by the anti-PSA antibody on the immune substrates. Then, the substrates was covered with 10 μl of 4MBA-Ag NRs@SiO₂ immune probes solution and incubated at room temperature for 3 h. Subsequently, the substrate was consecutively rinsed with TBS/0.05% Tween®20 buffer solution, TBS and deionized water to remove exceed unbound probes. Lastly, the whole sandwich structure was dried in the argon gas and used for SESR measurement.

Instruments

Absorption spectra were measured by using an UV-Vis spectrometer (TU-1901, Pgeneral). Transmission electron microscope (TEM) and high-resolution transmission electron microscope (HRTEM) images were obtained using a TEM (JEM-2100F, JEOL) operated at accelerating voltage of 200 kV. SERS signals were measured by using a Raman spectrometer (BWS415, B&W Tek Inc.) which is equipped with a semiconductor laser (785-nm, 499.95 mW), the dispersed grating of 1200 lines·mm⁻¹ and the charge-coupled device (CCD) (2,048×2,048 pixels) detector.

Results and discussion

Properties of Ag NRs and 4MBA-Ag NRs@SiO₂

The typical TEM and HRTEM images of the as-prepared Ag NRs are shown in Fig. 1. From Fig. 1(a), the Ag NRs prepared at 0.02 M CTAB exhibit an average diameter of 30 ± 3 nm and an average length of 60 ± 6 nm, corresponding to the aspect ratio of ~2. In Fig. 1(b), the as-prepared Ag NRs have an average diameter of 15 ± 2
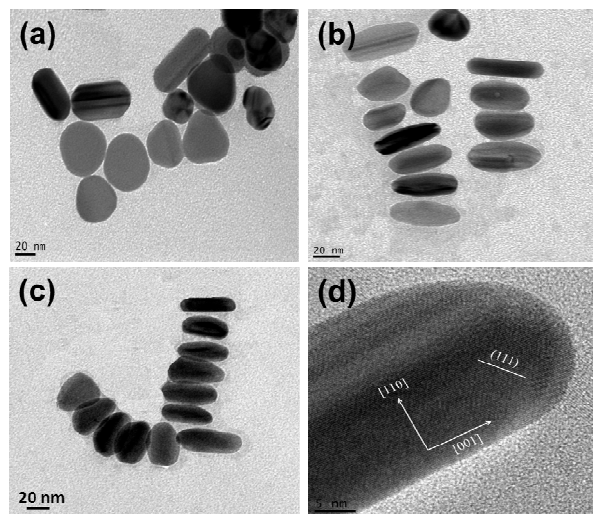
nm, an average length of 50 ± 4 nm and the aspect ratio of 3.3. Compared with Fig. 1(a), it can be seen that the number of Ag NRs has a significant increase when the concentration of CTAB was increased to 0.05 M. In Fig. 1(c), the Ag NRs display an average diameter of 20 ± 2 nm, an average length of 42 ± 4 nm and the aspect ratio of 2.1. The results are suggested that the Ag NRs obtained at 0.05 M CTAB has a better morphology comparing to the Ag NRs prepared at 0.02 and 0.08 M CTAB. In Fig. 1(d), it is clearly display that the Ag NRs are single-crystalline structure with {111} facets and growing along the [001] direction.
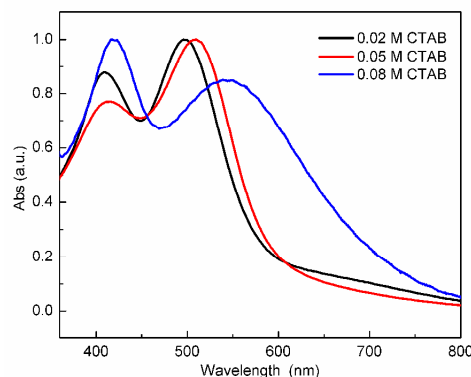

Fig. 2 UV-Vis absorption spectra of Ag NRs obtained at different concentrations of CTAB

The normalized absorption spectra of the CTAB concentration-dependent Ag NRs are shown in Fig. 2. It can be seen that the localized surface plasmon resonance (LSPR) band of Ag NRs obtained at 0.02 M CTAB is consisted of longitudinal plasmon resonance (LPR) band located at 497 nm and the transverse plasmon resonance (TPR) band at about 409 nm. And the full width at half maximum (FWHM) of the TPR and LPR band are about 40 and 50 nm, respectively. In the case of 0.05 M CTAB, the LPR band of Ag NRs red-shifted to 509 nm and the TPR band remained almost at their original position, which indicates a larger aspect ratio of Ag NRs. Besides, the FWHM of TPR band narrowed to 30 nm and FWHM of LPR band broaden to 55 nm. The narrowed FWHM of TPR band indicated the size distribution of Ag NRs became narrower because the as-prepared Ag NRs is more homogenous. The broaden FWHM of LPR band implies the aspect ratio of as-prepared Ag NRs increased obviously. From Fig. 1(a) and 1(b), it also can be seen that the size distribution of Ag NRs is narrower than that of Ag NRs obtained at 0.02 M CTAB. For the case of 0.08 M CTAB, the LPR band of as-prepared Ag NRs exhibits a considerable red-shift with a FWHM of 80 nm and its TPR band remained the same position and has a stronger intensity than the LPR band. It implies that the structure of Ag NRs tends to be oblate rods,[24] as shown in Fig. 1(c). The surfactant CTAB plays a key role on the stability and dispersibility of Ag NRs, but the excess CTAB molecules in a colloid solution are free molecules which exhibit significant toxicity to biological tissue.[25] Thus, a purification step is necessary to obtain functionalized Ag NRs. As described in section "Preparing of Ag NR", the Ag NRs solution was purified by centrifugation washing step, so that an optimal number of centrifugation cycles are essential to maximize the stability and the functionalization of Ag NRs. The

Fig. 1 TEM images of Ag NRs prepared at (a) 0.02 M, (b) 0.05M and (c) 0.08M CTAB. (d) HRTEM image of Ag NR prepared at 0.05 M CTAB.

absorption spectra of CTAB-coated Ag NRs were measured to reveal the structural transition in the CTAB layer and determine the optimal number of centrifugation cycles. The time-dependent absorption spectra of Ag NRs with centrifugation once and twice are displayed in Fig. 3(a) and 3(b), respectively. In Fig. 3(a), the TPR band at 417 nm remained approximately at their position, but the LPR band red-shifted from 511 nm to 539 nm after 9 h, owing to the aggregation of Ag NRs with less CTAB surfactant by one centrifugation cycle. And the LPR band of Ag NRs suffered a considerable blue shift to 491 nm after 36 h because of the precipitation of Ag NRs aggregates in the bottom of container and the decrease of the average size of the nanoparticles in solution. It is agreement with the explanation of the reference.[26] As a comparison, the TPR band exhibited a slight red-shift from 410 nm to 420 nm, while the LPR band almost disappeared after 9 h as shown in Fig. 3(b). Moreover, it is clearly show that the absorption spectrum of Ag NRs at 36 h is almost completely overlapped with the absorption spectrum at 9 h, which indicates the majority of Ag NRs have been aggregated and precipitated on the bottom of the container at 9 h after centrifugation twice, owing to the loss protection of CTAB. Therefore, the subsequent removal of CTAB resulted in a loss of stability of the Ag NRs after going through one washing step, and one centrifugation cycle was selected as an optimal washing step in our following-up experiments.
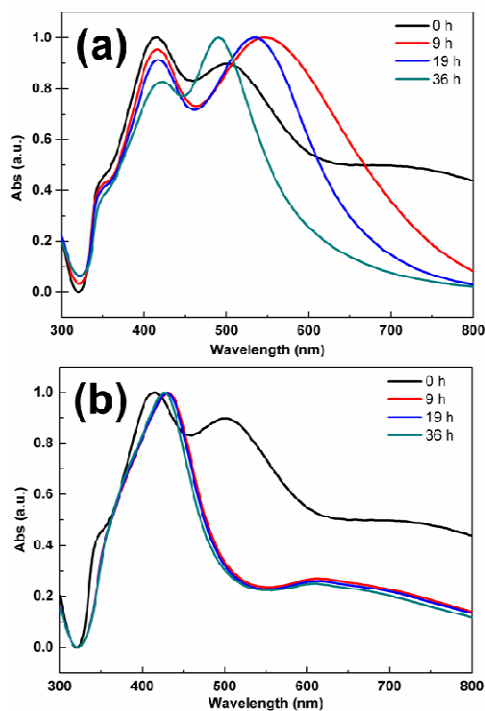

Fig. 4 TEM images of (a) sample 1, (b) sample 2 and (c) sample 3. The insets are corresponded to single 4MBA-Ag NRs@SiO₂ in their TEM images. (d) UV-Vis absorption spectra of sample 1 (curve a), sample 2 (curve b), and sample 3 (curve c)

concentration of CTAB increased to 0.08 M, because the controlled hydrolysis and condensation of TEOS are difficult to achieve on the surfaces of Ag NRs for more remaining CTAB monolayers,[27] as shown in Fig. 4(c). In addition, UV-vis absorption spectra of 4MBA-Ag NRs@SiO₂ were also measured and shown in Fig. 4(d) to investigate its optical properties. In Fig. 4(d), curve a, b and c are corresponding to the absorption spectra of the samples 1, 2 and 3, respectively. In Fig. 4(d), the absorption spectrum of sample 1 clearly displayed the red-shift of LPR band at 510 nm, but the position of TPR band almost fixed. It is because the LPR band of Ag NRs is highly sensitive to the particle size and the optical refractive index of the surrounding environment.[21] The absorption spectra of sample 2 and 3 show only one LSPR band located at about 420 nm, which demonstrates that the 4MBA-Ag NRs@SiO₂ are of quasi-spherical shapes due to the aggregation of Ag NRs during their preparation process.[28]

SERS activity of the 4MBA-Ag NRs@SiO₂

To investigate the SERS activity of the 4MBA-Ag NRs@SiO₂, the Raman spectra of samples 1, 2 and 3 were measured under the conditions of 10 s integration time and 49 mW of laser power and shown in Fig. 5. As a controlled experiment, the SERS spectrum of 4MBA-tagged Ag NRs is also included in Fig. 5. It is well known that the two dominant Raman peaks of 4MBA molecules at 1078 cm⁻¹ and 1585 cm⁻¹ are assigned to ring-breathing modes of 4MBA.[29] And, the SERS signal intensity of the 4MBA-Ag NRs@SiO₂ is much stronger than that of 4MBA-tagged Ag NRs, which implies that the 4MBA-Ag NRs@SiO₂ could be used as an excellent SERS-based immune probe because the "hot spots" of the aggregated Ag NRs in the 4MBA-Ag NRs@SiO₂ lead to a great enhancement of Raman signal.[30] In addition, to evaluate the repeatability, five independent measurements per sample type have been performed

Fig. 3 Time-dependent UV-Vis spectra of Ag NRs submitted to the centrifugation cycles from once (a) to twice (b)

The typical TEM images of samples 1, 2 and 3 are shown in Fig. 4. It can be seen that, from Fig. 4(a), the Ag NRs has been successfully coated by a thin silica shell with 3±1 nm. As the concentration of CTAB increased to 0.05 M, the thickness of the silica shell increased to 6 nm as shown in the inset of Fig. 4(b). And the thickness of the silica shell slightly decreased as the
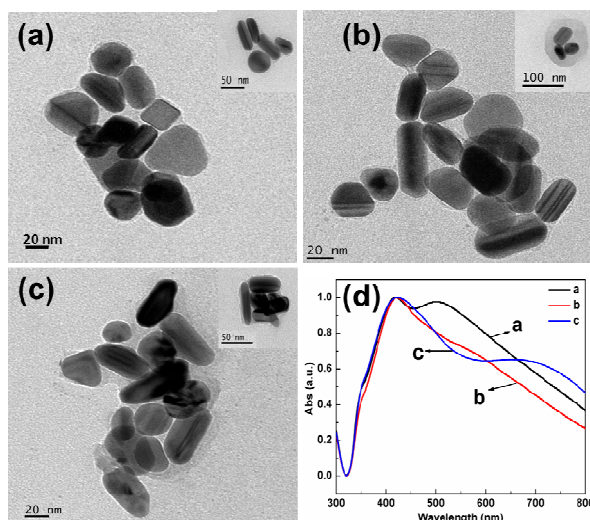
and the results are shown in Fig. S2. It can be concluded that the SERS spectra of as-prepared samples exhibit excellent repeatability.
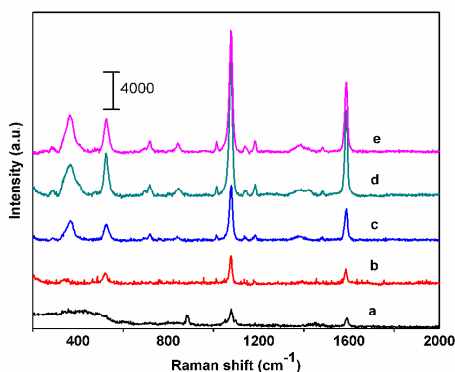

Fig. 5 Raman spectra of (a) 4MBA solutions, (b) 4MBA-tagged Ag NRs, and (c) sample 1, (d) sample 2, and (e) sample 3

As an important evaluation of the SERS enhancement ability, the Raman enhancement factor (*EF*) of 4MBA-Ag NRs@SiO$_2$ was calculated by using the following equation:[31]

$$EF = \frac{I_{SERS}N_{bulk}}{I_{bulk}N_{SERS}} \qquad (1)$$

where I_{SERS} and I_{bulk} are the integrated intensities of the same Raman band in the SERS and bulk Raman spectra, respectively; N_{bulk} is the number of molecules probed in the bulk sample; and N_{SERS} is the number of 4MBA molecules adsorbed on the surfaces of Ag NRs. In our study, the integrated area of the peak at 1078 cm^{-1} is selected to calculate the value of EF. The N_{bulk} of the 4MBA solution (10 mM)

is calculated to be 1×10^{11} for an illuminated volume 4.51 μm^3. The N_{SERS} of sample 1 is calculated to be 1.7281×10^4 for an illuminated volume 3.83 μm^3. And, as shown in Fig. 5, the I_{SERS} of sample 1 and the I_{bulk} of the 4MBA solution are 1.43×10^6 and 9.31×10^4, respectively. Thus, the *EF* value of sample 1 was 9.1×10^7. Same as to the above, the *EF* values of sample 2 and 3 are calculated to be 1.58×10^8 and 1.43×10^8, respectively. Furthermore, the *EF* value of Ag NRs is 4.4×10^7. It is obvious that the sample 2 has a better SERS performance than the other samples due to its higher aspect ratio of Ag NRs and more hot-spots between Ag NRs.[32, 33]

High sensitive immunoassay

According to the immunoassay protocol described in section "Immunoassay protocol", the SERS spectra of 4MBA corresponding to the different concentrations of PSA from 0.3 fg·ml^{-1} to 0.3 μg·ml^{-1}, including the background baseline without PSA, were measured and shown in Fig. 6(a). It is clearly shows that the SERS intensity of 4MBA molecules gradually increases with increasing concentrations of PSA, and the SERS signal of the blank sample is very weak. The dose-response data of the peak intensity at 1078 cm^{-1} is list in Tab. S1 and can be fitted by a linear fitting equation y = 23059.68733 + 1425.96983x. As shown in Fig. 6(b), the peak intensity are approximately proportional to the concentration of PSA and the limit of detection is as low as 0.3 fg·ml^{-1} (8.824×10^{-18} mol/L).

In addition, the reproducibility and reliability of PSA immunoassay was also experimentally examined. The SERS spectra of 4MBA corresponding to 3 μg·ml^{-1} of PSA concentration were recorded by averaging five readings of the signals at 8 random spots on the sample substrate under the same measure conditions and shown in Fig.6(c). Fig. 6(d) presents the peak intensities at 1078 cm^{-1} measured at the above mentioned 8 spots, and an average intensity
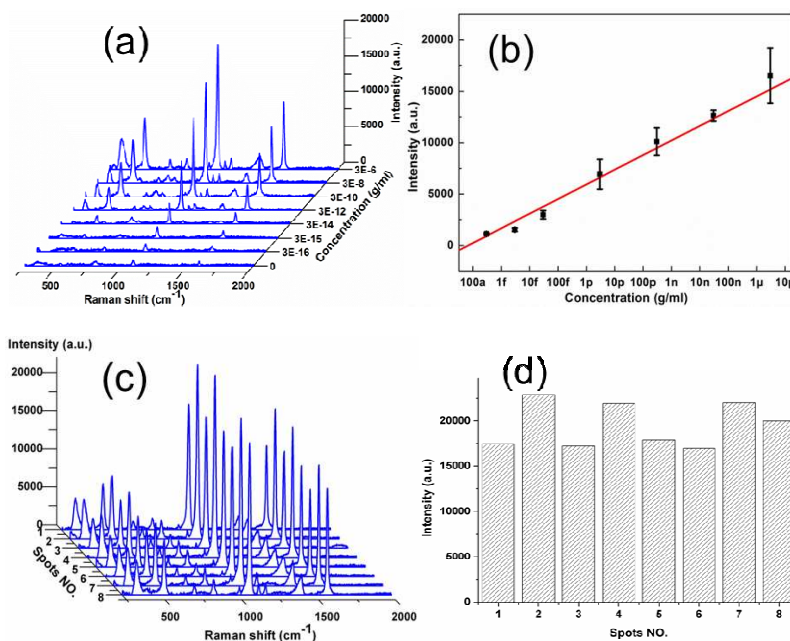

Fig. 6 (a) SERS spectra of 4MBA at different PSA concentrations, (b) the dose-response curve of the peak intensity at 1078 cm^{-1} with PSA concentration, (c) SERS spectra of 4MBA at 8 random spots on the substrate corresponding to the PSA concentration 3 μg·ml^{-1}, and (d) the peak intensities at 1078 cm^{-1}.

value of ~ 19675.3238 ± 2348.656984 is obtained with significance level α = 0.05. It demonstrated the SERS-based immunoassay protocol has excellent reliability for the detection of PSA.

On the other hand, the selectivity of this immunoassay protocol was also checked. The apolipoprotein B, as a contrast protein instead of PSA, was selected to examine the specific binding of anti-PSA antibody immobilized on the SERS-active immune substrate and 4MBA-Ag NRs@SiO$_2$ immune probe. As illustrated in Fig. 7, the characteristic SERS signal of 4MBA obtained from the contrast test (red curve) is weak and similar to that of the blank sample without PSA (black curve), comparing with that of 4MBA for the detection of PSA (blue curve). Thus, non-specificity was confirmed between the apolipoproptein B and the SERS-immune substrate as well as the 4MBA-Ag NRs@SiO$_2$ immune probe. Therefore, the immunoassay
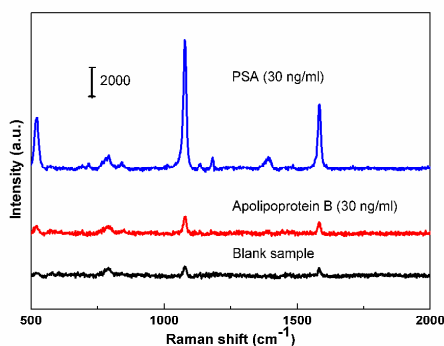

Fig.7 SERS signal of 4MBA for the 30 ng·ml^{-1} target antigens which were PSA (blue curve, upper), apolipoprotein B (red curve, centre), and the lower black curve represent the SERS of the blank sample without PSA.

protocol exhibits an excellent selectivity for the detection of PSA.

Conclusions

The as-prepared core-shell nanostructure 4MBA-Ag NRs@SiO$_2$, which consisted of thin silica shell and Ag NRs aggregates core with 4MBA, has displayed experimentally its excellent SERS performance. As an immune probe, the 4MBA-Ag NRs@SiO$_2$ synthesized at 0.05 M CTAB exhibits *EF* value of 1.58×10^8 which is higher than that of other samples prepared at 0.02 and 0.08 M CTAB, respectively. In our experiment, a sandwich-type SERS-based immunoassay protocol was successfully designed to detect tumour marker PSA. The experimental results presented that the SERS signal of 4MBA depends on the concentrations of PSA and an ultra-sensitivity with the limit of detection 0.3 fg·ml^{-1} (8.824×10^{-18} mol/L). It demonstrated that the as-prepared of 4MBA-Ag NRs@SiO$_2$ can be used as "building block" of biosensor platform and has potential applications for the early detection of prostate cancer.

Acknowledgements

Reference

1 Y. Arata and A. Shimizu, *Biochemistry*, 1979, **18**, 2513-2520.
2 I. Hwang, K. Yoo, J. Park, Y. Nam, I. Lee, J. Kang and M. Won, *Neuroscience*, 2004, **126**, 871-877.
3 B. Gu, C.Xu, C. Yang, S. Liu and M. Wang, *Biosens. Bioelectron.*, 2011, **26**, 2720-2723.
4 Q. Lang, F. Wang, L. Yin, M. Liu, V. Petrenko and A. Liu, *Anal. Chem.*, 2014, **86**, 2767-2774.
5 J. Gong, Y. Liang, Y. Huang, J. Chen, J. Jiang, G. Shen and R. Yu, *Biosens. Bioelectron.*, 2007, **22**, 1501-1507.
6 H. Ahmed and H. M. E. Azzazy, *Biosens. Bioelectron.*, 2013, **49**, 478-484.
7 J. Luo, X. Cui, W. Liu and B. Li, *Spectrochim. Acta A*, 2014, **131**, 243-248.
8 S. Xu, Y. Liu, T. Wang and J. Li, *Anal. Chem.*, 2011, **83**, 3817-3823.
9 E. Sharif, J. Kiely and R. Luxton, *J. Immunol. Methods.*, 2013, **388**, 78-85.
10 F. Jung, H. H. D. Meyer and R. T. Hamm, *J. Agr. Food Chem.*, 1989, **37**, 1183-1187.
11 D. S. Wright, H. B. Halsall and W. R. Heineman, *Anal. Chem.*, 1986, **58**, 2995-2998.
12 H. H. Jeong, N. Erdene, J. H. Park, D. H. Jeong and H. Young, *Biosens. Bioelectron.*, 2013, **39**, 346-351.
13 C. L. Haynes, A. D. McFarland and R. P. Van Duyne, *Anal. Chem.*, 2005, **77**, 338A-346A.
14 L. Shu, J. Zhou, X. Yuan, Z Jia and P. Mormile, *Talanta*, 2014, **123**, 161-168.
15 Y. Cui, B. Ren, J. Yao, R. Gu and Z. Tian, *J. Raman Spectrosc.*, 2007, **38**, 896-902.
16 J. Du, and C. Jing, *J. Phys. Chem. C*, 2011, **115**, 17829-17835.
17 S. S. R. Dasary, A. K. Singh, D. Senapati, H. Yu and P. C. Ray, *J. Am. Chem. Soc.*, 2009, **131**, 13806-13912.
18 T. Jiang, L. Zhang and J. Zhou, *Analyst*, 2014, **139**, 5894-5901.
19 Y. Sun, B. Mayers and Y. Xia, *Adv. Mater.*, 2003, **15**, 641-646.
20 C. M. Sturgeon and A. R. Ellis, *Clin. Chim. Acta*, 2007, **381**, 85-92.
21 C. J. Murphy and N. R. Jana, *Adv. Mater.*, 2002, **14**, 80-82.
22 W. Zhang, X. Qiao, Q. Chen, Y. Cai and H. Chen, *Appl. Surf. Sci.*, 2012, **258**, 5909-5913.
23 Y. Kobayashi, H. Katakami, E. Mine, D. Nagao, M. Konno and L. M. Liz-marzán, *J. Colloid Interf. Sci.*, 2005, **283**, 392-396.
24 C. Sonnichsen, T. Franzl, T. Wilk, G. Von Plessen, J. Feldmann, O. Wilson and P. Mulvaney, *Phys. Rev. Lett.*, 2002, **88**, 077402-077402.
25 Y. Ma, J. Zhou, L. Shu, T. Li, L. Petti and P. Mormile, *J. Nanopart. Res.*, 2014, **16**, 2439.
26 N. W. Dennis, B. B. Muhoberac and J. C. Newton, A. Kumbhar and R. Sardar, *Plasmonics*, 2014, **9**, 111-120.
27 I. Pastoriza-Santos, J. Pérez-Juste, L. M. Liz-Marzán, *Chem. Mater.*, 2006, **18**, 2465-2467.
28 Y. Cao, R. Zheng, X. Ji, H. Liu, R. Xie and W. Yang, *Langmuir*, 2014, **30**, 3876-3882.
29 S. W. Bishnoi, C. J. Rozell, C. S. Levin, M. K. Gheith, B. R. Johnson, D. H. Johnson and N. J. Halas, *Nano Lett.*, 2006, **6**, 1687-1692.
30 G. Gu, J. Kim, L. Kim and J. S. Suh, *J. Phys. Chem. C*, 2007, **111**, 7906-7909.
31 R. A. Álvarez-Puebla, *J. Phys. Chem. Lett.*, 2012, **3**, 857-866.

ARTICLE

32 C. J. Orendorff, L. Gearheart, N. R. Jana and C. J. Murphy, *Phys. Chem. Chem. Phys.*, 2006, **8**,165-170.
33 H. Xu, E. J. Bjerneld, M. Kll and L. Borjesson, *Phys. Rev. Lett.*, 1999, **83**, 4357-4360.

Analytical Methods Accepted Manuscript
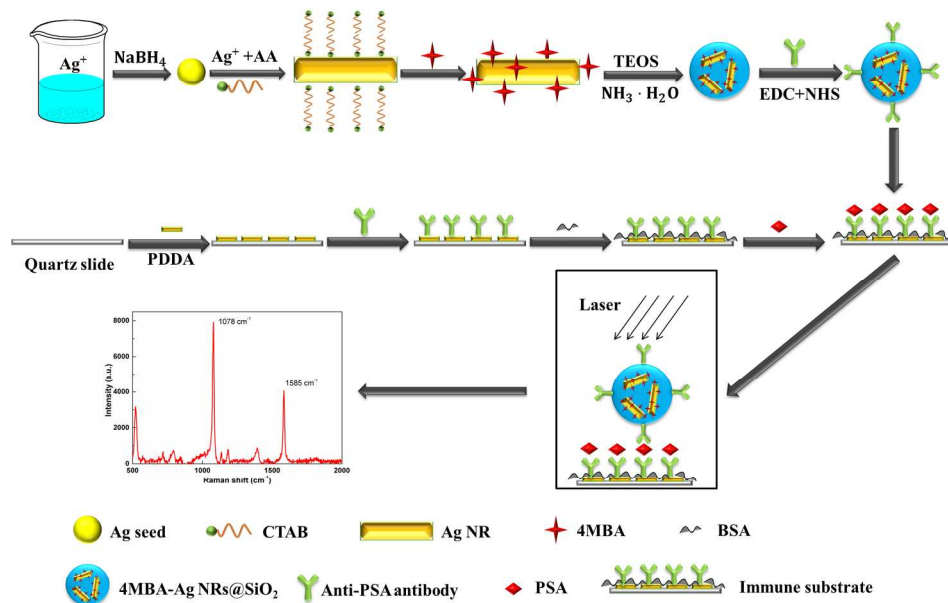
Schematic representation of the immunoassay protocol

374x259mm (150 x 150 DPI)